with enhanced electron density in the more peripheral portions. This is a characteristic difference of bonding and anti-bonding orbitals. Although this may be the expected behavior, again it is not necessary that every $\pi-\pi$ redistribution give a red shift since the basic functional groups may not be affected or the nodal properties may actually deplete the electron density at the basic sites.

The red shifts observed for the proton donors may be rationalized. All of these data refer to the transitions corresponding to the $A_{1g} \rightarrow B_{2u}$ transition of benzene, a transition to an excited state containing nodal planes perpendicular to the plane of the ring. The red shift suggests that this orbital places a nodal plane through the H-bonding functional group, so as to reduce the electron density at this site. This would cause an acidic group to become a better proton donor. Aromatic acids (phenol, aniline) should display red shifts whereas aromatic bases (anisole, dimethylaniline) should display no shift in basic solvents (as is observed, see ref. 1) and a blue shift in acidic solvents (no data available).

Conclusions

It seems clear that the solvent shifts caused by H-bonding solvents contain interesting information. In addition to empirical correlations which may aid in establishing the type of transition, these solvent shifts provide clues to the locale and nature of electron redistribution in the electronic transition. Perhaps the unique aspect is the promise for understanding the electronic distribution and H-bonding properties of excited states. For this purpose absorption and emission studies should be combined, if possible, to give the shift corresponding to the O–O transition.

Acknowledgment.—The author wishes to thank Dr. M. Kasha and Dr. Sydney Leach for helpful and critical comments on the subject matter of this paper.

BERKELEY 4, CALIF.

[CONTRIBUTION FROM THE SCHOOL OF CHEMISTRY, UNIVERSITY OF MINNESOTA]

Equations for the Limiting Current at the Rotated Dropping Mercury Electrode[1]

BY YUTAKA OKINAKA AND I. M. KOLTHOFF

RECEIVED JANUARY 26, 1957

This paper describes results of a theoretical and experimental study of the relationship between the limiting current at the rotated dropping mercury electrode on the one hand and the diffusion coefficient of the electroactive species, the kinematic viscosity of the solution, and the characteristics of the electrode on the other. Two theoretical equations are derived on the basis of hydrodynamics, one for the case when no surface-active substance is present and the other for the case when such substances are present. In view of the fact that the presence of a suitable surface-active substance is necessary for most practical purposes, the relations in the presence of a capillary-active substance were studied more extensively than those in its absence. The proposed equation in the presence of surface-active compounds involves an experimentally determined numerical constant and yields satisfactory agreement between observed and calculated limiting currents in the range of 75 to 210 r.p.m., provided that an electrode of the proper dimensions is employed. At a suitable speed of rotation in the presence of a surface-active substance, the limiting current at the rotated dropping mercury electrode, as a first approximation, is proportional to $D^{2/3}(mt)^{1/2}$, while at the unrotated conventional dropping mercury electrode it is proportional to $D^{1/2}m^{2/3}t^{1/6}$. Limitations of the derived equations are discussed both from theoretical and practical viewpoints.

The rotated dropping mercury electrode (R.D.M.E.) recently developed in this Laboratory[2] is of practical importance because it allows polarographic determinations at concentrations of an order of magnitude of one smaller than with the conventional dropping mercury electrode (D.M.E.). The quantitative dependence of the limiting current upon various factors is quite different at these two electrodes. In the present paper the results of a theoretical and a systematic practical study of the factors which affect the limiting current at the R.D.M.E. are described. In order to determine the effect of the height of mercury on the limiting current, it was necessary to revise the construction of the electrode previously described.[2] The expressions derived at 25° for the average limiting current in the absence (eq. 1) and presence of a surface-active compound which completely suppresses stirring at the mercury surface (eq. 2) are

$$i_l = 230nCD^{1/2}\{m^{2/3}t^{1/6} + 103D^{1/2}(mt)^{1/3} + 7.45U_0^{1/2}(mt)^{1/2}\} \quad (1)$$

$$i_l = 230nCD^{1/2}\{m^{2/3}t^{1/6} + 103D^{1/2}(mt)^{1/3} + 5.76U^{1/2}\nu^{-1/6}D^{1/6}(mt)^{1/2}\} \quad (2)$$

where i_l is the average limiting current in μa., n the number of electrons involved in the electrochemical reaction, C the concentration of the electroactive species in mM, D the diffusion coefficient in cm.^{2}/sec., m the rate of flow of mercury in mg./sec., t the drop time in sec., U_0 the uniform velocity of the solution at the surface of the mercury drop in cm./sec., U the speed of rotation of the electrode in cm./sec. and ν the kinematic viscosity of the solution in cm.^{2}/sec. In the presence of surface-active substances satisfactory agreement between calculated (eq. 2) and observed limiting currents was found only when the electrode has a relatively small orifice (<0.75 mm. in diameter) and a small distance between the orifice and center of rotation (<8.5 mm.).

As shown in this paper, the first and second

(1) This research was supported by the United States Air Force through the Air Force Office of Scientific Research of the Air Research and Development Command under contract No. AF18(600)-1516. Reproduction in whole or in part is permitted for any purpose of the United States Government.

(2) W. Stricks and I. M. Kolthoff, THIS JOURNAL, **78**, 2085 (1956)

terms are much smaller than the third term in the brackets of both equations 1 and 2 when U_0 or U is not very small. Therefore, as a rough approximation, we can write

$$i_l \sim nCD^{1/2}U_0^{1/3}(mt)^{1/2} \quad (1a)$$

$$i_l \sim nCD^{2/3}U^{1/2}\nu^{-1/6}(mt)^{1/2} \quad (2a)$$

If we compare these relationships with the Ilkovic equation at the D.M.E.

$$i_d = 607nCD^{1/2}m^{2/3}t^{1/6}$$

the following noticeable differences between the two types of electrodes are evident: (1) the effect of the height of mercury is much smaller at the R.D.M.E. than at the D.M.E., because at the former the product mt is practically constant with varying height of mercury, (2) the effect of applied potential and hence drop time t is much larger at the R.D.M.E. ($\sim t^{1/2}$) than at the D.M.E. ($t^{1/6}$), (3) in the presence of a surface-active substance i_l is not proportional to $D^{1/2}$ at the R.D.M.E., but closely to $D^{2/3}$.

Theoretical

When the current is controlled by diffusion and the effect of electrical migration is eliminated, the current at an instant, t, in the reduction (or oxidation) of an electroreducible (or oxidizable) substance is generally expressible by

$$i_t = nFD\iint_S \left(\frac{\partial c}{\partial x}\right)_{x=0,t} dS \quad (3)$$

where F is the faraday, S the area of the electrode, c the concentration at distance x from the electrode surface. As far as mass transfer is the only process controlling the current, the above fundamental equation is applicable to the R.D.M.E. if the concentration gradient at the surface of the electrode is explicitly expressible. According to the so-called "Nernst diffusion layer" concept,[3] when an electrode is placed in a stirred solution, there exists at the surface of the electrode a thin diffusion layer in which there is no motion of the solution. In view of the known fact that this simple assumption is not generally justified in stirred solutions,[3] it is necessary to apply hydrodynamic principles in order to take into account the effect of convection on mass transfer. Assuming that a mercury drop is a perfect sphere at any instant, the general equation of mass transfer[3] is given by

$$\frac{\partial c}{\partial t} = D\left(\frac{\partial^2 c}{\partial r^2} + \frac{2}{r}\frac{\partial c}{\partial r} + \frac{1}{r^2}\Delta c\right) - \left(v\frac{\partial c}{\partial r} + \frac{u}{r}\frac{\partial c}{\partial \theta} + \frac{w}{r\sin\theta}\frac{\partial c}{\partial \phi}\right) \quad (4)$$

where

$$\Delta = \frac{1}{\sin\theta}\frac{\partial}{\partial\theta}\left(\sin\theta\frac{\partial}{\partial\theta}\right) + \frac{1}{\sin^2\theta}\frac{\partial^2}{\partial\phi^2}$$

v, u and w are the velocity components in r, θ and ϕ directions, respectively. The spherical coördinates were chosen as shown in Fig. 1. Making suitable assumptions to obtain the concentration gradient at the mercury surface, equation 4 was solved, which allowed the calculation of the current using equation 3.

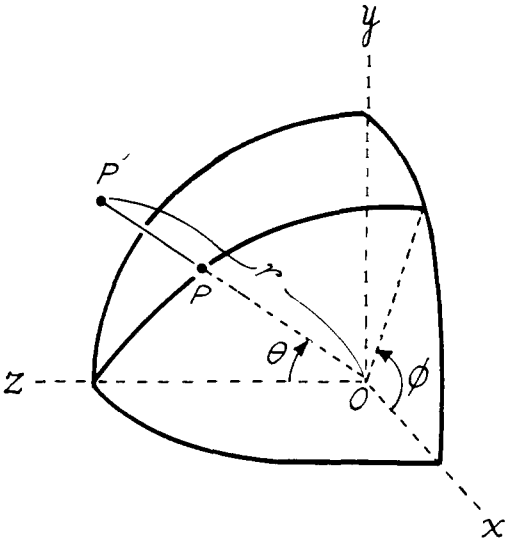

Fig. 1.—Spherical coördinates for equation 4.

When a mercury drop is moved in an aqueous solution, two extreme situations can be considered at the mercury surface. One is the case in which flow velocities do not vanish; in other words, the solution slips on the mercury surface. This phenomenon occurs when the solution does not contain surface-active substances.[4] The other is the case in which flow velocities vanish on the mercury surface. Frumkin and Levich[5] showed that when a mercury drop falls into a solution containing a surface-active substance, the slip of the solution on the mercury surface is partly or completely inhibited by the formation of an elastic film of the surface-active substance on the mercury drop. These two different situations on the mercury surface are relevant to the experimental results at the rotated dropping amalgam electrode introduced by Stricks and Kolthoff.[2] They found that the limiting anodic current at a rotated dropping thallium amalgam electrode increases with rate of rotation in the absence of gelatin but remains unaffected by the speed of rotation in its presence. The larger current at higher speeds of rotation in the absence of gelatin is considered to be caused by the fact that the tangential flow on the amalgam surface enhances a motion within the amalgam drop, whereas in the presence of gelatin this motion does not occur since there are no flow velocities on the amalgam surface. We shall deal with these two cases separately, for they are entirely different from the hydrodynamic viewpoint. The following theoretical statements are made by considering for the sake of convenience that the electrode is placed in a solution flowing at a speed of U, instead of considering that the electrode is moved at this speed in the solution.

Case A.—The solution slips on the mercury surface, the situation in the absence of a surface-active substance.

(3) P. Delahay, "New Instrumental Methods in Electrochemistry," Interscience Publishers, Inc., New York, N. Y., 1954, Chapter 9.

(4) B. Levich, *Disc. Faraday Soc.*, 1, 37 (1947).

(5) A. Frumkin and B. Levich, *J. Phys. Chem., U.S.S.R.*, **21**, 1183 (1947).

The initial and boundary conditions for equation 4 in this case are

$$c = C \text{ when } t = 0 \quad (5)$$

$$c = 0 \text{ at } r = R(t) \text{ when } t > 0 \quad (6)$$

in which $R(t)$ is the radius of the mercury drop at the time t. Condition (6) implies that the electrode reaction takes place instantaneously when the electroactive species reaches the mercury surface. Equation 1 was derived with the assumption that the electrode interface is completely mobile and the velocity at any point on the mercury surface is uniformly equal to U_0, which is different from the apparent speed of rotation of the electrode. A complete description of the derivation of equation 1 is given in Appendix 1.

Case B.—The solution does not slip on the mercury surface; the situation in the presence of a surface-active substance.

If there is no slip of the solution on the electrode surface as in the case of a solid placed in a moving fluid, there must be a velocity gradient between the surface of the electrode and the bulk of the solution. The type of flow around the mercury drop can be estimated by evaluating the Reynolds number, $Re = Ul/\nu$, where l is the length representing the dimension of the electrode, which may be taken to be equal to the diameter of the mercury drop. For example, for one of our suitable electrodes the distance between the orifice and the center of rotation, d, was 0.74 cm. and the weight of a drop of mercury 0.037 g. at 210 r.p.m. The linear speed of rotation, U, of this electrode is calculated to be about 16 cm./sec., and the diameter of a mercury drop 0.13 cm. just before it is ejected from the orifice. Putting these values and 0.9×10^{-2} cm.^{2}/sec. as ν of water at 25° in the Reynolds number expression, Re is calculated to be equal to 230. Provided that there is no significant disturbance in the character of flow caused by the part of the glass end tube of the electrode dipped in the solution, it is considered from this Reynolds number that there will be a laminar boundary layer around the mercury drop, at least after it has grown to some extent.[6] However, at the very beginning of the growth of a mercury drop, when its size is small, the Reynolds number is certainly very small and the type of flow is considered to be rather close to Stokes' motion. This stage is of short duration and the type of flow will soon become laminar with a boundary layer. For example, the Reynolds number of the above electrode becomes 100 at 0.9 sec. with a drop life of 3.1 sec. Thus it is reasonable to assume that the type of flow is that with a laminar boundary layer during most of the drop life.

In order to solve equation 4 with this assumption, it is necessary to have expressions for the velocity distribution in the boundary layer and for its thickness, δ. Assuming a curvilinear system of coordinates (Fig. 2), whose x-axis is in the direction of the wall, the y-axis being perpendicular to it, the Prandtl boundary layer equations for steady flow[7] generally are given by

$$u\frac{\partial u}{\partial x} + v\frac{\partial u}{\partial y} = -\frac{1}{\rho}\frac{dp}{dx} + \nu\frac{\partial^2 u}{\partial y^2} \quad (7)$$

$$\frac{\partial u}{\partial x} + \frac{\partial v}{\partial y} = 0 \quad (8)$$

where u and v are the velocity components in x- and y-directions, respectively, ρ the density of the solution and p the pressure. Assuming that the velocity of flow outside the boundary layer around the small mercury drop is uniformly equal to the speed of rotation of the electrode, U, equations 7 and 8 can be solved by analogy to the case of a flat plate.[8] In view of the known fact that the tangential velocity distribution can be successfully approximated by a parabolic or polynomial function with respect to δ and y,[8] we shall make the further assumption that it is given by a polynomial of nth degree, which can be written as

$$u = U - U(\delta - y)^n/\delta^n \quad (9)$$

Prescribing the boundary conditions

$$u = 0, v = 0 \text{ where } y = 0 \quad (10)$$

$$u = U \text{ where } y = \delta \quad (11)$$

$$\delta = 0 \text{ where } x = 0 \quad (12)$$

we obtain the following expression for δ from (7), (8) and (9) (the mathematical process follows the case of a flat plat[8])

$$\delta = \sqrt{2(2n+1)(n+1)\nu x/U} \quad (13)$$

Thus if a parabolic distribution is assumed, *i.e.*, $n = 2$, we obtain

$$\delta = \sqrt{30\nu x/U} \quad (14)$$

The numerical constant of 30 in equation 14 must be determined experimentally because there is no theoretical support for the above velocity distribution. Somewhat arbitrarily we adopt the value of 30 in the mathematical treatment, a complete description of which is given in Appendix 2.

For case B the initial and boundary conditions for equation 4 are

$$c = C \text{ when } t = 0 \quad (15)$$

$$c = 0 \text{ at } r = R(t) \text{ when } t > 0 \quad (16)$$

$$c = C \text{ at } r = R(t) + \delta \text{ when } t > 0 \quad (17)$$

in which conditions 15 and 16 are the same as in case A and condition 17 implies that the concentration outside the boundary layer is always kept equal to the bulk concentration. Under these conditions we obtain the following equation for the limiting current at 25° in the presence of a surface active substance

$$i_l = 230nCD^{1/2}\{m^{2/3}t^{1/6} + 103D^{1/2}(mt)^{1/3} + KU^{1/2}\nu^{-1/6}D^{1/6}(mt)^{1/2}\} \quad (18)$$

where K becomes equal to 5.38, 5.82, 6.00 or 6.10 depending on whether the tangential velocity distribution is assumed to be a linear, a parabolic, a third or a fourth degree polynomial.

Experimental

Materials.—Conductivity water and 99.99% pure Linde nitrogen and C.P. chemicals were used without further puri-

(6) The transition from laminar to turbulent flow takes place at $Re = 3 \times 10^5$ in the case of a sphere. See, for example, H. Schlichting, "Boundary Layer Theory," translated by J. Kestin, McGraw-Hill Book Co., Inc., New York, N. Y., 1955, p. 34.

(7) Ref. 6, pp. 94-99.

(8) Ref. 6, pp. 201-206.

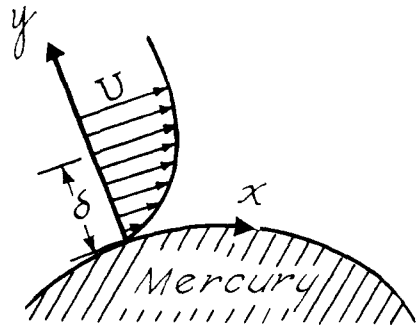

Fig. 2.—Curvilinear coördinates for equations 7 and 8.

fication except thallous chloride, which was purified by recrystallization. Solutions of known concentration of thallium and lead were prepared by dissolving weighed amounts of thallous chloride or lead nitrate in the appropriate amount of water. A zinc solution of known concentration was prepared by dissolving a weighed amount of pure zinc in dilute sulfuric acid and adjusting the volume. A solution of known cadmium concentration was obtained by dissolving an approximately weighed amount of cadmium sulfate in water and weighing as anhydrous salt after evaporation of an appropriate volume of the solution and drying. Nickel(II) perchlorate was prepared by adding an excess perchloric acid to the nitrate and evaporating to dryness. The nickel content of a solution of the perchlorate was determined gravimetrically by weighing as nickel dimethyl glyoxime.

Current Measurements.—Limiting currents were measured with a Leeds and Northrup Electrochemograph Type E with damping switch in a suitable position,[2] and with a manual apparatus as described by Lingane and Kolthoff.[9] All experiments were carried out at 25.0 ± 0.1°. All reported values of limiting currents have been corrected for residual currents.

Measurements of Kinematic Viscosity.—In the experiments in the presence of glycerol and sucrose the kinematic viscosity was measured with Ubbelohde suspended level viscometers, which had been calibrated with standard glycerol-water mixtures.

Electrode.—The R.D.M.E. described by Stricks and Kolthoff[2] was modified so that the height of the mercury column could be varied. The construction and manipulation of the modified R.D.M.E. are similar to those of the original one. The top and bottom of the plunger of a 2-ml. syringe are cut off (see Fig. 3) and the resulting tube is connected by Tygon tubing to a top tube as used with a D.M.E.; this constitutes the upper part of the electrode. The lower part consists of two units. One of these is made by connecting an end tube to a capillary. The other unit consists of the outer tube of the syringe, the bottom of which has been cut off, joined to the wide end of the glass tube A (Fig. 3). The lower part of the electrode is assembled by placing the mercury filled end tube and capillary in the holder of the rotating apparatus, and by connecting the small end of the glass tube A to the capillary. After this part is positioned properly, it is filled with mercury up to the top and the upper part of the electrode is connected through the two syringe pieces. The syringe is so well ground that the rotation is completely smooth; the height of mercury can be raised to about 100 cm. from the tip of the end tube without leakage of mercury. A detailed description concerning the treatment of the end tube with Silicone Dri Film and the rotating device is in the previous paper.[2] Eccentric rotation must be avoided.

The lower part of the end tube was 50 mm. in length and had an outside diameter of 3.5 to 4 mm. (see Fig. 3). The distance between the orifice and the bottom of the end tube was about 10 to 12 mm. for all electrodes used in the present experiments. The diameter of the orifice varied from 0.4 to 1.1 mm.; the distance between the orifice and center of rotation, d, was from 5 to 16 mm.

The electrolysis vessel used was a beaker of 250 ml. capacity. The volume of the solution was 100 ml. in all experiments.

(9) J. J. Lingane and I. M. Kolthoff, THIS JOURNAL, **61**, 825 (1939).

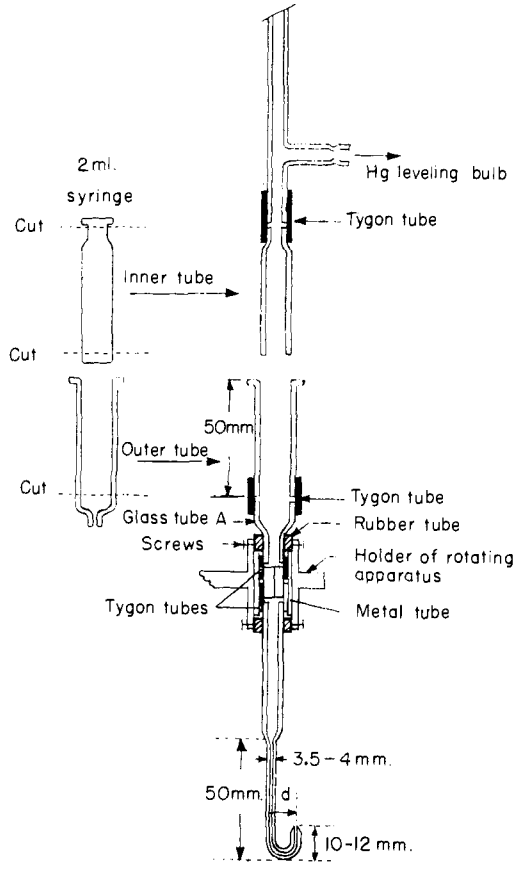

Fig. 3.—Assembly of the modified R.D.M.E.

General Characteristics of the Modified R.D.M.E. Relationship between the Height of Mercury, h, and m and t.—The general characteristics of the electrode were determined by using the same capillary with three different end tubes. The capillary used was 3.5 cm. in length of Sargent's capillary for D.M.E., the drop time of which was specified as 2 to 5 sec. The diameter of the orifice ϕ was measured with a microscope provided with an eye-piece micrometer. The distance between the orifice and center of rotation, d, was measured with a micrometer caliper. The results are listed in Table I, in which h is the height of mercury corrected for

TABLE I

GENERAL CHARACTERISTICS OF THE MODIFIED R.D.M.E. DETERMINED IN 1 M $NaClO_4$ WITH AN OPEN CIRCUIT AT 210 R.P.M.

End tube	d, mm.	ϕ, mm.	h, cm.	m,[a] mg./sec.	t, sec.	mt, mg.	m/h	ht
1	8.74	1.0	91.4	20.26	2.56	51.9	0.222	234
			61.4	13.86	3.72	51.0	.226	228
			51.4	11.52	4.56	52.5	.224	234
2	6.93	1.1	91.4	20.29	3.34	67.7	.222	306
			61.4	13.81	4.84	66.9	.225	298
			51.4	11.55	5.78	66.9	.225	298
3	7.31	0.75	91.3	20.21	1.91	38.6	.221	174
			61.3	13.81	2.77	38.3	.225	170
			51.3	11.53	3.31	38.1	.225	170

[a] The m values were determined without rotation.

back pressure,[10] $h_{back} = 3.1/(mt)^{1/4}$ cm. This expression was derived from the fundamental formula $P_{back} = 2\sigma/r$ which gives the difference in pressure between outside and inside of a spherical surface of a liquid whose surface tension

(10) I. M. Kolthoff and J. J. Lingane, "Polarography," Vol. 1, Interscience Publishers, Inc., New York, N. Y., 1952, pp. 79–81.

is σ and radius r, and is applicable immaterially whether the tip of the electrode is upward or downward. Table I shows that (1) m is proportional to h, (2) t is inversely proportional to h, (3) m is entirely controlled by the characteristics of the capillary, and is not affected by the end tube and (4) the weight of a drop of mercury, mt, is practically constant with changing height of mercury.

Results and Discussion

Case A. Absence of a Surface-active Substance.—By putting actual numerical values in equation 1 the sum of the first and second terms becomes less than 10% of the third term when U_0 is not too small. For example, when m = 15 mg./sec., t = 3 sec., $D = 10^{-5}$ cm.^{2}/sec., n = 1, C = 0.1 millimole/l. and U_0 = 15 cm./sec., the first, second and third terms are calculated to be equal to 0.53, 0.03 and 9.59 μa., respectively. Thus if we neglect the first and second terms, equation 1 becomes

$$i_l = 1714nCD^{1/2}U_0^{1/2}(mt)^{1/2} \qquad (19)$$

The relationship involved in this equation accounts for the following experimental facts: (1) i_l/n is proportional to C and to $D^{1/2}$. This has been found to be the case[2]; (2) i_l is nearly independent of the height of mercury, because mt is constant with varying height of mercury. Experimentally this relationship was found to be obeyed, as is illustrated by one example in Table II.

TABLE II

LIMITING CURRENTS AT DIFFERENT HEIGHTS OF MERCURY IN THE ABSENCE OF SURFACE-ACTIVE SUBSTANCES

(End tube 3, 0.400 millimole/l., Tl^+ in 1 M $NaClO_4$, 210 r.p.m.)

V (*vs.* S.C.E.)	i_l (μa.) h = 93.5 cm.	h = 63.5 cm.
−0.7	44.0	43.2
−0.9	43.3	43.1
−1.1	42.8	42.8
−1.3	41.0	41.4
−1.5	38.0	38.5
−1.7	34.5	34.5

In the derivation of equation 1, we made an assumption that the velocity of flow on the mercury surface is uniformly equal to U_0. This surface velocity is not simply equal to the speed of rotation of the electrode, U, as there are complications caused by the viscosity of a real fluid, which exerts frictional forces on the mercury–solution interface, and by the mutual interaction between the motion inside the mercury drop and the tangential motion of the solution on the mercury surface. The presence of even trace amounts of surface active substances in the solution lowers the limiting current. At potentials other than the electrocapillary zero, the existence of an electrical double layer exerts a viscous drag resulting from the forces acting on the two sheets of the double layer and decreases the mobility of the interface.[11] Since the actual surface velocity is unknown, a direct comparison between calculated and observed limiting currents cannot be made.

Levich[4] derived the following equation for currents involving maxima of the second kind at the D.M.E. with the assumption that the electrode interface is completely mobile

$$i = 8nFC\sqrt{\pi/2}\sqrt{DU_0/R}\,R^2$$

in which R is the radius of a given spherical drop. Apparently this equation was derived for an unexpanding liquid electrode. If we substitute R with $(3mt/4\pi d)^{1/3}$ where d is the density of mercury, and evaluate the average limiting current, we obtain

$$i_l = (1/t)\int_0^t i\,dt = 2710nCD^{1/2}U_0^{1/2}(mt)^{1/2}$$

where i_l is expressed in terms of μa. This equation is identical with equation 19 except for the numerical constant.

Case B. Presence of a Surface-active Substance. Relation between i_l and t.—A number of experiments were carried out with several different end tubes and capillaries at various heights of mercury at 210 r.p.m. in solutions of 0.400 mM in thallous ion and 1 M sodium perchlorate in the presence of 0.01% gelatin. Some typical examples of plots of log i_l *vs.* log t using different end tubes and different capillaries are given in Figs. 4 to 6. The limiting currents were measured at various applied potentials, and hence at various drop times, the other conditions being kept constant. The points obtained with end tube 2 (Fig. 4) were scattered in a somewhat irregular way, but with the other end tubes reasonably good straight lines were obtained at voltages between −0.7 and −1.6 v. *vs.* S.C.E. It is seen that the slope increases with the diameter ϕ of the orifice, and hence with the drop weight mt. Equation 2 or 18 predicts that the slope should be close to 0.5, because under our experimental conditions the sum of the first and second terms is of the order of only 15% or less of the third term (for some numerical examples, see Table IV). The theoretical relationship is obeyed approximately with end tube 3 which has a relatively small orifice. The deviation in the slope from 0.5 for the other end tubes with larger orifice must be attributed to the deformation of the shape of a mercury drop from a sphere.

Experimental Determination of K in Equation 18.—As mentioned in the theoretical part, we made the assumption that the tangential velocity distribution is parabolic or polynomial in the boundary layer. Since this assumption affects only the numerical constant K, we must find the proper value of K experimentally. This was performed by comparing experimental values of limiting currents with theoretical values calculated from equation 18 where K tentatively was put equal to 5.82 (corresponding to a parabolic distribution).

In the calculation of limiting currents, it is important to use correct D values which were determined under the actual experimental conditions. The D values at infinite dilution calculated from equivalent conductance data are often quite different from those under the working conditions in polarography, although they are frequently used with the original Ilkovic equation for the D.M.E. In connection with the development of revisions of the original Ilkovic equation, several

(11) A. Frumkin and B. Levich, *Acta physicochim. U.R.S.S.*, **20**, 769 (1945).

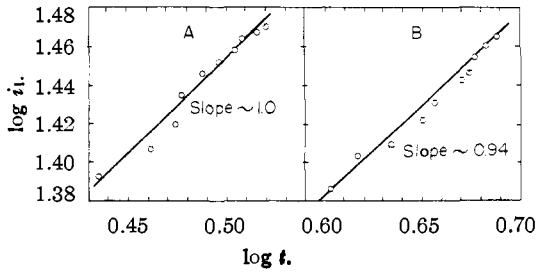

Fig. 4.—Limiting current *vs.* drop time at 210 r.p.m. (0.4 m*M* Tl^+ in 1 *M* $NaClO_4$ and 0.01% gelatin; end tube 2, ϕ = 1.1 mm., d = 6.93 mm.). (A) capillary 3, h = 60.6 cm., m = 20.77 mg./sec., mt at −0.7 v. *vs.* S.C.E. = 69.0 mg. (B) capillary 1, h = 62.2 cm., m = 13.81 mg./sec., mt at −0.7 v. *vs.* S.C.E. = 67.5 mg.

attempts have been made recently to determine diffusion coefficients independently by the radiotracer technique,[12,13] the Cottrell technique in connection with a proposal of a new modified Ilkovic equation[14] and the diaphragm-cell technique.[15] However, the reported values, as summarized in Table III, do not agree with each other. Since

TABLE III

DIFFUSION COEFFICIENTS OF METAL IONS AT 25°

Ion	Supporting electrolyte	Wang, *et al.*[a]	$D \times 10^5$, cm.²/sec. Stackelberg, *et al.*[b]	Rulfs[15]	Infinite dilution[c]
Tl^+	0.1 *M* KCl	1.827	1.744	1.67	2.00
	0.005 *M* KCl	1.92	1.91[d]	..	
Pb^{++}	1 *M* KCl	1.001	0.920	..	0.98
	0.1 *M* KCl	0.970	.867	0.75	
Cd^{++}	0.1 *M* KNO_3	...	.690	0.76	0.72
Zn^{++}	1 *M* KNO_3	0.73	.619	..	0.72
	0.05 *M* KNO_3	.69	.653	..	
	2 *M* KCl	.940	.743	..	
	1 *M* KCl	.818	.723	..	
	0.1 *M* KCl	.729	.673	..	
	.01 *M* KCl	.712[d]	.676	..	
Ni^{++}	.1 *M* $NaClO_4$ + .001 *M* $HClO_4$	.60 (by Sanborn and Orlemann[13])			0.69

[a] Determined in the presence of 0.0005 *M* $[H^+]$ except for Tl^+. Ref. 12a and 12b. [b] Determined in the presence of 0.1% acetic acid except for Tl^+ and 0.01% gelatin. Ref. 14. [c] Ref. 10, p. 52. [d] Estimated by an interpolation of the curve $D - \sqrt{c}$ (c is concentration of the supporting electrolyte).

there are three different D values reported for thallous ion in 0.1 *M* potassium chloride, we carried out a series of experiments with 0.404 mmole/l. thallous ion in 0.1 *M* potassium chloride in the presence of 0.01% gelatin at 210 r.p.m. and calculated K by comparing observed and theoretical limiting currents using each of the three D values. The experiments were conducted with end tube 3 which has a small orifice. This end tube is suitable for theoretical studies because the deformation from a sphere of the growing drop is small. An

(12) (a) J. H. Wang, THIS JOURNAL, **76**, 1528 (1954); (b) J. H. Wang and F. M. Polestra, *ibid.*, **76**, 1584 (1954).

(13) R. H. Sanborn and E. F. Orlemann, *ibid.*, **77**, 3726 (1955).

(14) M. v. Stackelberg, M. Pilgram and V. Toome, *Z. Elektrochem.*, **57**, 343 (1953).

(15) C. L. Rulfs, THIS JOURNAL, **76**, 2071 (1954).

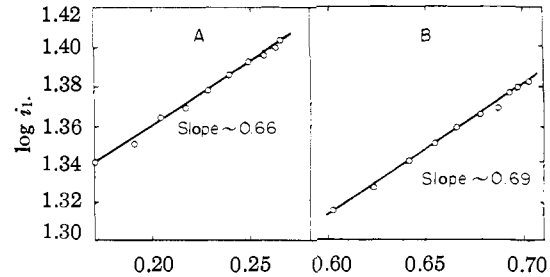

Fig. 5.—Limiting current *vs.* drop time at 210 r.p.m. (0.4 m*M* Tl^+ in 1 *M* $NaClO_4$ and 0.01% gelatin; end tube 4, ϕ = 0.9 mm., d = 6.55 mm.). (A) capillary 3, h = 75.6 cm., m = 26.90 mg./sec., mt at −0.7 v. *vs.* S.C.E. = 49.5 mg. (B) capillary 4, h = 63.5 cm., m = 9.60 mg./sec., mt at −0.7 v. *vs.* S.C.E. = 48.7 mg.

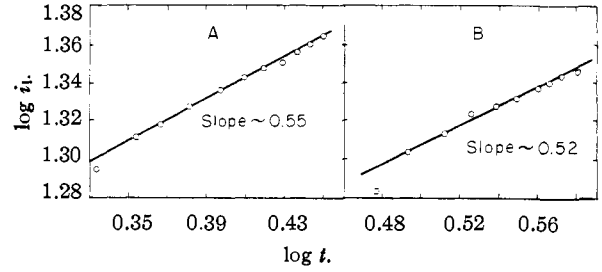

Fig. 6.—Limiting current *vs.* drop time at 210 r.p.m. (0.4 m*M* Tl^+ in 1 *M* $NaClO_4$ and 0.01% gelatin; end tube 3, ϕ = 0.75 mm., d = 7.31 mm.). (A) capillary 1, h = 62.2 cm., m = 13.81 mg./sec., mt at −0.7 v. *vs.* S.C.E. = 38.2 mg. (B) capillary 4, h = 63.5 cm., m = 9.70 mg./sec., mt at −0.7 v., *vs.* S.C.E. = 36.8 mg.

example of sets of calculated and observed values is shown in Table IV. The last column of Table IV is the experimental factor which should be multiplied by the tentative value of K, 5.82, in equation 18. In the calculation of limiting cur-

TABLE IV

DETERMINATION OF K

(0.404 m*M* Tl^+ in 0.1 *M* KCl, 0.01% gelatin. End tube 3, 210 r.p.m.)

Capillary no.	h, cm.	m, mg./sec.	V *vs.* S.C.E.	t, sec.	i_l obsd., μa.	Calcd. values (μa.) 1st term	2nd term	3rd term	x[a]
1	72.2	15.87	−0.7	2.36	23.5	2.89	0.58	20.21	0.991
			−1.0	2.28	22.8	2.88	.58	19.86	.974
			−1.3	2.13	21.9	2.84	.56	19.20	.964
			−1.5	2.00	21.1	2.81	.55	18.61	.953
1	52.2	11.47	−0.7	3.24	23.0	2.46	0.58	20.13	0.992
			−1.0	3.13	22.5	2.44	.58	19.79	.984
			−1.3	2.90	21.2	2.41	.56	19.04	.957
			−1.5	2.76	21.1	2.39	.55	18.58	.977
4	78.5	12.10	−0.7	3.12	23.3	2.53	0.59	20.29	0.995
			−1.0	2.95	22.9	2.51	.58	19.72	1.005
			−1.3	2.74	21.9	2.48	.56	19.01	0.992
			−1.5	2.57	20.9	2.45	.55	18.42	.972
4	63.5	9.77	−0.7	3.79	22.7	2.27	0.58	20.09	0.988
			−1.0	3.62	22.1	2.25	.57	19.64	.982
			−1.3	3.36	21.3	2.22	.56	18.92	.979
			−1.5	3.14	20.6	2.20	.55	18.29	.976
4	53.5	8.21	−0.7	4.49	22.3	2.07	0.58	20.04	0.981
			−1.0	4.28	21.6	2.06	.57	19.57	.969
			−1.3	4.00	20.8	2.03	.56	18.92	.962
			−1.5	3.71	20.2	2.01	.55	18.23	.968

[a] $x = \{i_l(\text{obsd.}) - (\text{1st} + \text{2nd terms})\}/(\text{3rd term})$, $K = 5.82x$.

TABLE V
COMPARISON OF OBSERVED AND CALCULATED LIMITING CURRENTS OF SEVERAL METAL IONS
(End tube 3, capillary 4, 210 r.p.m.)

Ion	Supporting electrolyte	$\nu \times 10^2$, cm.²/sec.	C, mM	m, mg./sec.	V	t, sec.	i_l (obsd.), μa.	i_l (calcd.), μa. K:5.76[a]	K:5.97[b]	K:6.16[c]
Tl^{+g}	0.005 M KCl	0.898	0.101	6.68	−0.9[d]	5.45	5.59	5.71	5.82	..
Pb^{++h}	1 M KCl	.853	.502	9.86	−0.7[e]	3.99	39.0	39.4	38.5	..
	0.1 M KCl	.892	.507	12.19	−0.7[e]	3.24	38.6	39.3	37.7	35.3
Cd^{++h}	0.1 M KNO_3	.887	.460	12.19	−0.8[e]	3.24	31.0	30.4[f]	29.5	32.2
Zn^{++h}	1 M KNO_3	.825	.400	9.83	−1.3[e]	3.47	24.6	24.1	22.3	..
	0.05 M KNO_3	.894	.400	6.66	−1.5[d]	5.43	22.7	23.4	22.9	..
	2 M KCl	.825	.400	9.86	−1.45[e]	3.29	28.2	28.0	24.6	..
	1 M KCl	.853	.400	9.86	−1.35[e]	3.40	25.4	25.6	24.4	..
	0.1 M KCl	.892	.400	12.19	−1.2[e]	3.02	25.6	25.0	24.5	..
	.01 M KCl	.898	.200	9.84	−1.3[d]	3.72	11.8	12.1	12.0	..
Ni^{++h}	.1 M $NaClO_4$ + 0.001 M $HClO_4$	.897	.378	9.86	−1.3[e]	3.52	20.3	19.9[f]	20.5[i]	21.1

[a] With the D values reported by Wang, *et al.* (Table III). [b] With the D values reported by Stackelberg, *et al.* (Table III). [c] With the D values reported by Rulfs (Table III). [d] *Versus* mercury pool anode. [e] *Versus* S.C.E. [f] Using the D value reported by Rulfs (Table III). [g] In the presence of 0.01% gelatin. [h] In the presence of 0.01% starch. [i] Using the D value reported by Sanborn and Orlemann (Table III).

rents, 0.892×10^{-2} cm.²/sec. was used as the kinematic viscosity of 0.1 M potassium chloride and a value of $D = 1.827 \times 10^{-5}$ cm.²/sec. as reported by Wang and Polestra. This example shows that the factor x was practically constant with varying m and t. The same was found also when other D values were used. We repeated two more sets of experiments and determined K from a total of 56 measurements of limiting currents, all of which were obtained with the same end tube at 210 r.p.m., but with various capillaries at various heights of mercury. The average values of x were calculated to be 0.990 ± 0.021, 1.025 ± 0.021 and 1.059 ± 0.022 with D values of 1.827×10^{-5}, 1.744×10^{-5} and 1.67×10^{-5} cm.²/sec., respectively. By multiplying 5.82 by these x values, the average values of K became 5.76, 5.97 and 6.16, respectively. These K values are used in Table V for the calculations of the limiting currents of ions different from thallium.

Typical experimental data in Table IV also show that the effect of the height of mercury on the limiting current is much smaller than at the D.M.E. as predicted from the theoretical equation because $(mt)^{1/6}$ in the third (principal) term of the equation is constant with varying height of mercury.

Comparison of Observed and Calculated Limiting Currents of Several Metal Ions with Different Diffusion Coefficients.—In order to examine the validity of the proposed equation with respect to the relationship between i_l and D, several experiments were carried out with solutions of thallium, lead, cadmium, zinc and nickel at various concentrations of supporting electrolytes. The experiments were conducted with end tube 3 and capillary 4 at 210 r.p.m. In the experiments with heavy metal ions starch was used as a surface-active substance instead of gelatin because a small fraction of the heavy metals is bound by gelatin.[2] Starch is not bound by the heavy metal ions and 0.01% was found sufficient to suppress completely maxima of the second kind. The kinematic viscosities were calculated from densities and specific viscosities, which were taken from the International Critical Tables, or measured with an Ubbelohde viscometer.

The observed and calculated limiting currents are tabulated in Table V. Using the above three values of K the calculated values of limiting currents were obtained by employing the various values of D listed in Table III. The best agreement between calculated and observed values was obtained with diffusion coefficients determined by the radiotracer technique. This result lends support to the reliability of the D values determined by this technique and to the conclusion that reliable values of D can be derived from measurements with the R.D.M.E. The good agreement between the theoretical value of K of 5.82 and the experimental value of 5.76 indicates that the average tangential velocity distribution in the boundary layer is closely approximated by a parabolic function. v. Stackelberg, Pilgram and Toome[14] determined their values of D in the presence of gelatin for all of the ions used in the present experiments, while we did not use gelatin except for thallous ion. This accounts, in part at least, for the lower values of the limiting currents calculated with their D values.

Results Obtained with Various End Tubes at Various Speeds of Rotation.—The validity of the proposed equation 18 was further tested with respect to the correlation between i_l on the one hand and m, t and U on the other. Experiments were carried out with solutions of thallous ion in 1 M sodium perchlorate, 0.05 M potassium nitrate and 0.1 M potassium chloride in the presence of 0.01% gelatin.

The tracer diffusion coefficients of thallous ion in sodium perchlorate and potassium nitrate are not available in the literature. However Wang[12a] and Wang and Polestra[12b] concluded from experimental results that observed diffusion currents at a D.M.E. agree better with values calculated from the Strehlow-Stackelberg equation[16,17]

$$i_d = 607nCD^{1/2}\{m^{2/3}t^{1/6} + AD^{1/2}(mt)^{1/3}\}$$

where A is equal to 17, or more accurately 16.7, than with values calculated from the original

(16) H. Strehlow and M. v. Stackelberg, *Z. Elektrochem.*, **54**, 51 (1950).

(17) O. H. Müller, Natl. Bur. Stand. Circular 524, Aug. 14 (1953).

TABLE VI

COMPARISON OF OBSERVED AND CALCULATED LIMITING CURRENTS OF Tl^+ IN THE PRESENCE OF 0.01% GELATIN AT VARIOUS ELECTRODES

End tube	d, mm.	ϕ, mm.	C, mM	Capillary r.p.m.		h, cm.	m, mg./sec.	V vs S.C.E.	t, sec.	i_l (obsd.), μa.	i_l (calcd.), μa.
2	6.93	1.1	0.400	210[a]	3	75.6	25.63	−0.7	2.66	29.7	29.9
								−1.3	2.40	27.6	28.5
					1	52.2	11.55	−0.7	5.86	29.2	28.5
								−1.3	5.37	26.6	27.3
4	6.55	0.9	.402	300[b]	4	64.0	9.80	−0.7	3.66	25.0	25.1
								−1.3	3.26	23.2	23.8
			.400	210[a]	3	75.6	26.90	−0.7	1.84	25.3	25.4
								−1.3	1.65	23.4	24.2
					4	78.5	11.84	−0.7	4.11	24.2	23.9
								−1.3	3.69	22.3	22.8
3	7.31	.75	.402	600[b]	4	35.8	5.46	−0.7	2.17	16.8	20.9
								−1.3	1.96	14.8	19.9
			.400	210[a]	1	92.2	20.29	−0.7	1.92	23.1	23.4
								−1.3	1.66	21.6	21.9
					4	53.5	8.14	−0.7	4.51	22.1	21.6
								−1.3	4.00	21.0	20.5
			.400	150[a]	4	93.5	13.87	−0.7	3.25	20.6	21.1
								−1.3	2.87	19.5	20.0
						53.5	8.15	−0.7	5.56	20.4	20.6
								−1.3	4.92	19.1	19.4
			.400	75[a]	4	93.5	13.87	−0.7	4.03	17.2	17.5
								−1.3	3.59	16.4	16.6
							8.15	−0.7	6.87	16.7	16.8
								−1.3	6.11	16.0	16.0
6	6.58	.42	1.00	210[a]	5	87.3	8.92	−0.7	2.92	43.8	44.6
								−1.3	2.60	40.9	41.9
5	6.32	.35	1.00	210[a]	5	60.2	6.15	−0.7	3.33	38.0	38.2
								−1.3	2.98	36.4	36.2
7	5.16	.5	0.392	210[a]	6	90.2	7.79	−0.7	4.48	17.7	17.7
								−1.3	4.00	16.9	16.8
10	8.46	.5	.404	210[c]	5	75.0	7.47	−0.7	3.42	20.5	20.1
				150[c]	5	75.0	7.47	− .7	4.19	19.4	19.1
				75[c]	5	75.0	7.47	− .7	5.31	15.7	15.8
9	10.54	.7	.404	150[c]	4	78.0	12.00	− .7	3.87	24.4	25.8
				75[c]	4	78.0	12.00	− .7	4.90	20.3	21.4
8	15.98	.7	.404	150[c]	5	90.0	9.02	− .7	4.02	24.9	27.4
				75[c]	5	90.0	9.02	− .7	5.60	20.6	23.5

[a] In 1 M $NaClO_4$ ($\nu = 0.870 \times 10^{-2}$ cm.^{2}/sec.). [b] In 0.05 M KNO_3 ($\nu = 0.894 \times 10^{-2}$ cm.^{2}/sec.). [c] In 0.1 M KCl ($\nu = 0.892 \times 10^{-2}$ cm.^{2}/sec.).

Ilkovic equation ($A = 0$)[18] and the Lingane–Loveridge equation ($A = 39$),[18] when tracer diffusion coefficients are used for D. In accordance with the above conclusion, we calculated the diffusion coefficient of thallous ion in the given media from the diffusion current data obtained with a D.M.E. and the Strehlow–Stackelberg equation. The D values of thallous ion in 1 M sodium perchlorate and in 0.05 M potassium nitrate thus calculated are 1.74×10^{-5} and 1.85×10^{-5} cm.^{2}/sec., respectively.

Experimental and calculated limiting currents are listed in Table VI. With end tubes 2 and 4, which have a large orifice, the differences between the observed and calculated values at −1.3 v. were consistently more negative than those at −0.7 v. probably as a result of deviation from a sphere of a drop. The observed values with end tubes 3, 6, 5, 7 and 10 at 210, 150 and 75 r.p.m. are in agreement within a few per cent. with the calculated values at both of the applied potentials. The diameter of the orifice of these end tubes varied between 0.35 and 0.75 mm., and the distance between the orifice and center of rotation varied between 5.2 and 8.5 mm. At 600 r.p.m. with end tube 3, the observed results failed to fit the equation. A possible reason for this discrepancy is that the fraction of the surface area of the mercury drop inside the orifice and therefore not in contact with the solution at a higher speed of rotation is greater than at a lower speed of rotation, because the ejected mercury drops are smaller at a higher speed of rotation than those at a lower speed of rotation because of centrifugal force effects. The main reason for the discrepancy found at high speeds of rotation is attributed to the effect of the motion of the solution caused by the vigorous rotation of the electrode. We assumed in the derivation of the proposed equation that the velocity of outer flow is equal to the apparent speed of rotation; in other words, the electrode rotates in a medium at rest. Actually, however, especially at a high speed of rotation, the

(18) Ref. 10, pp. 34–46.

TABLE VII

EFFECT OF THE KINEMATIC VISCOSITY ON THE LIMITING CURRENT OF THALLOUS ION IN THE PRESENCE OF 0.01% GELATIN

(End tube 3, capillary 4, 210 r.p.m., m = 12.05 mg./sec.[a])

Wt. % glycerol	Supporting electrolyte	$\nu \times 10^2$, cm.²/sec.	$D \times 10^5$, cm.²/sec.	C_t, mM	V vs. S.C.E.	t, sec.	i_l (obsd.), μa.	i_l (calcd.), μa.
26.7	0.1 M KCl	1.827	0.968	0.804	−0.7	3.11	26.0	27.4
					−1.3	2.78	24.3	26.1
26.7	.05 M KNO_3	1.829	0.999	.804	−0.7	3.13	27.0	28.1
					−1.3	2.81	25.3	26.8
10.2	.05 M KNO_3	1.138	1.57	.804	−0.7	3.12	40.3	40.3
					−1.3	2.83	37.8	38.6
Sucrose								
30.9	0.05 M KNO_3	2.673	0.781	0.804	−0.7	3.10	21.8	22.6
					−1.3	2.80	20.6	21.6
14.2	.05 M KNO_3	1.309	1.34	.804	−0.7	3.11	35.4	35.6
					−1.3	2.80	33.0	33.9
0	.05 M KNO_3	0.894	1.85	.402	−0.7	3.13	23.7	23.3
					−1.3	2.79	22.3	22.1

[a] The m value was constant within the viscosity range investigated.

end tube serves as a stirrer giving rise to a swirling of the solution, and the solution moves in the same direction as the rotation of the electrode. Thus the velocity of rotation *relative* to the solution becomes smaller than the apparent speed of rotation and accounts for the fact that the calculated value of the limiting current is considerably greater than the experimental one. A similar effect is observed at the lower speeds of rotation when the distance between the orifice and center of rotation of the electrode is increased; this results in an effective swirling motion of the liquid caused by the rotation of the end tube. The effect is particularly pronounced with end tube 8 (d = 16 mm.) even at 75 r.p.m. and is still observed with end tube 9 (d = 10.5 mm). It is clear that for theoretical studies it is essential to choose an end tube of proper dimensions so that more or less well-defined and reproducible hydrodynamic conditions can be obtained.

Influence of the Kinematic Viscosity on the Limiting Current.—It is known that the diffusion current at the D.M.E. is greatly affected by the change of viscosity of the solution to be electrolyzed because of the variation of diffusion coefficients of electroactive species. In the case of the R.D.M.E., the viscosity of the solution is expected to exert an effect on the hydrodynamic boundary layer thickness in addition to the variation of the diffusion coefficient. This effect is related to the term $\nu^{-1/6}$ in equation 2. In order to examine the validity of the expected relation, experiments were carried out with thallous ion in 0.1 M potassium chloride and in 0.05 M potassium nitrate in the presence of 0.01% gelatin, the viscosity being varied by adding glycerol or sucrose.

Experimental and calculated limiting currents are tabulated in Table VII in which the values of D were calculated with the aid of the Strehlow–Stackelberg equation from the data obtained with a D.M.E. The equation was found valid when ν was varied from 0.89 to 1.3 × 10^{-2} cm.²/sec., but at higher viscosities the apparent effect of viscosity tended to become greater than expected from the equation. This is a natural result of the fundamental assumptions underlying the boundary layer theory itself. Prandtl's boundary layer, equations 7 and 8, on which our theoretical treatment is based, are derived from the general Navier–Stokes equations with the aid of the simplifications which can be introduced as a consequence of the small values of viscosity. This corresponds to the condition that the boundary layer thickness should be very small as is clear from the relation that the thickness of the boundary layer, δ, is proportional to $\nu^{1/2}$. From equation 14 the boundary layer thickness in 30.9% sucrose solution under the present experimental conditions, for example, is computed to be 0.83 mm. at 90° from the forward stagnation point just before the mercury drop comes off. This amounts to about a half of the maximum diameter of the mercury drop, 1.7 mm., which is contrary to our original assumption that δ is very small compared with the size of a mercury drop. The boundary layer theory is a limiting theory at zero viscosity, and the assumptions made in the derivation of the boundary layer equations are satisfied with an increasing degree of accuracy as the Reynolds number increases, *i.e.*, the viscosity decreases.[19] Thus it is to be expected that the proposed equation will also give more satisfactory results as the viscosity decreases.

A theoretical treatment may be possible also for the other limiting case of a very large viscosity. However, as is known from hydrodynamics, the experimental results at intermediate viscosities cannot be interpreted by an interpolation between the two limiting cases. In addition, the quantitative effect of the viscosity on the diffusion current at the D.M.E. is still incompletely known. Because of such difficulties, a quantitative interpretation of experimental results at moderately high viscosities is at present impossible.

Current–Time Relation during Individual Drop Life.—From equation 2 it follows that the equation of the instantaneous limiting current in the presence of a surface-active substance is given by

$$i_t = 230nCD^{1/2}\{(7/6)m^{2/3}t^{1/6} + (4/3)103D^{1/2}(mt)^{1/3} + (3/2)5.76U^{1/3}\nu^{-1/6}D^{1/6}(mt)^{1/2}\} \quad (24)$$

A few experiments were conducted to examine the validity of this equation. The current was measured in terms of the iR drop across a 10,000 ohm

(19) Ref. 6, p. 115.

standard resistor in series with the R.D.M.E. cell by using a fast response Sanborn Industrial Recorder, Model 127, combined with a preamplifier, Model 126. The maximum sensitivity of this instrument is 50 mv. per cm., and the paper was driven at a speed of 25 mm./sec. A manual polarograph was used to apply the constant voltage to the cell circuit.

Although the total applied voltage can be kept constant, the actual potential of the R.D.M.E. decreases as the drop grows because of the iR loss across the standard resistor. In the example given here, the maximum current was 18.1 μa., so that the decrease of the actual potential of the R.D.M.E. amounted to 0.181 v. However, as shown by Lingane[20] with a D.M.E., this magnitude of the variation in potential causes no perturbation of the current–time curves provided the total applied voltage is large enough to keep the potential of the R.D.M.E. in the limiting current region during the lifetime of a drop.

The present experiments were carried out with a 0.201 mM thallium solution in 0.05 M potassium nitrate in the presence of 0.01% gelatin with end tube 3 at 210 r.p.m. The m value was equal to 12.05 mg./sec. The total applied potential was −0.9 v. *vs.* S.C.E., and hence the potential of the R.D.M.E. decreased to −0.719 v. at the end of the drop life. An example of the current–time curve is shown in Fig. 7.

The disagreement between the observed and calculated current–time curves was significant in the region of early drop life. This trend is also observed with the D.M.E. Lingane[20] attributed it mainly to the variability of m during the drop life caused by the larger back pressure exerted on the young drop and also to the non-sphericity in the early life of the drop. In the case of the R.D.M.E. the variation of m is much smaller because the lumen of the orifice is larger than that of the capillary used with a D.M.E. For example, for the end tube used in the present experiment whose diameter of orifice is 0.75 mm., the back pressure calculated from the formula $P_{back} = 2\sigma/r$[10] amounts to *ca.* 1.7 cm. at the beginning and *ca.* 0.8 cm. at the end of the drop life. Therefore, from the expression $m = k(h - h_{back})$, the variation of m is calculated to be only *ca.* 2.5% when the height of mercury is kept at 40 cm.; this variation is too small to account for the difference between the experimental and theoretical curves in Fig. 7. With reference to the non-sphericity of the mercury drop, the deviation of the shape from a sphere at the early life of the drop is considered to be greater at the R.D.M.E. than at the D.M.E. because of the larger lumen of the orifice at the R.D.M.E. As the most important reason for the discrepancy, however, one cannot overlook the variation of the hydrodynamic conditions during the drop life. As mentioned in the theoretical part, at the beginning of the growth of the mercury drop, the Reynolds number is so small that the boundary layer theory fails to account for the hydrodynamic situation at the very early drop life. There is no doubt that a few mathematical simplifications are also responsible which

(20) J. J. Lingane, THIS JOURNAL, **75**, 788 (1953).

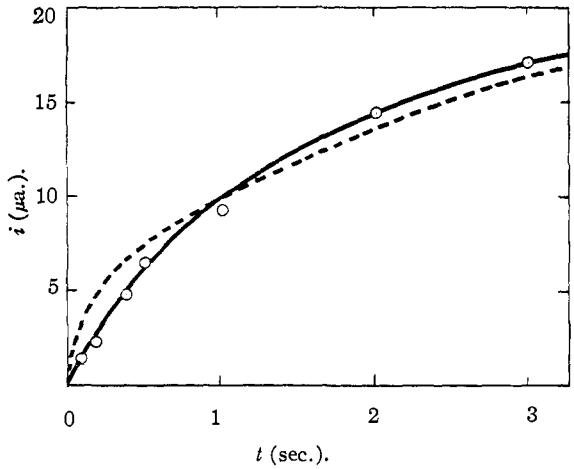

Fig. 7.—Current–time curve; end tube 3, capillary 4, 210 r.p.m., h = 78.5 cm., 0.201 mM, Tl^+ in 0.05 M KNO_3 and 0.01% gelatin; ———, experimental; - - -, theoretical.

were made for the purpose of obtaining a practical expression of the *average* limiting current.

We have discussed so far several aspects on the applicability of the proposed equation of the limiting current. Limitations of the equation are, of course, ascribed to the fact that some ideal situations were assumed which are somewhat different from the actual conditions. For example, the following assumptions are not fully justified even with an end tube whose dimension is in the recommended range; (1) the mercury drop is at any instant a perfect sphere which expands from its center outwards symmetrically, (2) the rotation of the electrode does not swirl the solution at all, (3) a laminar boundary layer is developed at any instant in the drop life, (4) the thickness of the boundary layer is expressed by the simple function (13). The fourth assumption is considered to be only a rough approximation from the purely hydrodynamic viewpoint, because it does not account for the separation of the boundary layer, which occurs on a body of revolution such as a sphere as a result of the acceleration in the front half and the deceleration in the rear half of the sphere. Since the expression for the boundary layer thickness was obtained by analogy with a flat plate, this assumption corresponds to a neglect of the curvature of the mercury drop as far as the boundary layer thickness is concerned. An attempt was made to make use of the expressions for the boundary layer thickness and the velocity distributions derived by taking the effect of curvature into consideration.[21] The final equation thus obtained is so involved and impractical that it is not given in this paper. At any rate, it is gratifying that only one numerical constant had to be determined empirically to obtain a satisfactory equation of the limiting current. It is considered that this empirical factor probably compensates on the average for the error resulting from the simplifications mentioned above.

Acknowledgment.—We wish to express our thanks to Dr. S. Ito of the Department of Mathe-

(21) Ref. 6, p. 165, p. 218.

matics of the University of Minnesota for his kind help in solving the differential equation.

Appendix 1 (Case A)

It is assumed throughout the following mathematical treatment that solutions to be electrolyzed are incompressible and the variation of c is marked only in the vicinity of the mercury surface.

Considering a spherical surface of radius r which is slightly larger than a growing mercury drop of radius $R(t)$, and letting the volume enclosed between the two spheres be ϵ, we have

$$4\pi r^3/3 = 4\pi\{R(t)\}^3/3 + \epsilon = 4\pi a^3 t/3 + \epsilon$$

where $a = (3m/4\pi d)^{1/3}$, d denoting the density of mercury. It follows from this that

$$3r^2 \frac{dr}{dt} = a^3$$

and hence

$$\frac{dr}{dt} = \frac{a^3}{3r^2} = \frac{1}{3r^2}\left(\frac{r^3 - 3\epsilon/4\pi}{t}\right)$$

When we consider the velocity of motion of a point on the spherical surface of radius r resulting from the growth of the mercury drop, it is clear that $r - R(t) << R(t)$ and $4\pi r^3/3 >> \epsilon$, and hence $dr/dt \cong r/3t$. Assuming that the r component of the flow velocity is negligible in comparison with the θ-component we get

$$v \cong r/3t \qquad \text{(A1)}$$

By putting $u = U_0$ and (A1) into equation 4 and neglecting w, we obtain

$$\frac{\partial c}{\partial t} = D\left(\frac{\partial^2 c}{\partial r^2} + \frac{2}{r}\frac{\partial c}{\partial r} + \frac{1}{r^2}\Delta c\right) - \frac{r}{3t}\frac{\partial c}{\partial r} - \frac{U_0}{r}\frac{\partial c}{\partial \theta} \qquad \text{(A2)}$$

Substituting the variables r and t by

$$\sigma = 3t^{1/3} \text{ and } \eta = r/at^{1/3}$$

equation (A2) becomes

$$\frac{\partial c}{\partial \sigma} = \frac{D}{a^2}\left(\frac{\partial^2 c}{\partial \eta^2} + \frac{2}{\eta}\frac{\partial c}{\partial \eta} + \frac{1}{\eta^2}\Delta c\right) - \frac{U_0\sigma}{3a\eta}\frac{\partial c}{\partial \theta}$$

Putting $\tau = D\sigma/a^2$, $\xi = \eta - 1$ and $f = \eta c/C$, we get from the above equation

$$\frac{\partial f}{\partial \tau} = \frac{\partial^2 f}{\partial \xi^2} + \frac{\Delta f}{(1+\xi)^2} - \frac{a^3 U_0 \tau}{3D^2(1+\xi)}\frac{\partial f}{\partial \theta} \qquad \text{(A3)}$$

Since the condition $r - R(t) << R(t)$ is equivalent to $\xi << 1$, we can put $1 + \xi \cong 1$. For the sake of simplicity, we put $A = a^3U_0/3D^2 = \text{const.}$ Then (A3) becomes

$$\frac{\partial f}{\partial \tau} = \frac{\partial^2 f}{\partial \xi^2} + \Delta f - A\tau\frac{\partial f}{\partial \theta} \qquad \text{(A4)}$$

By changing the variables as above, the initial and boundary conditions 5 and 6 become

$$f = 1 + \xi \text{ when } \tau = 0 \qquad \text{(A5)}$$

$$f = 0 \text{ when } \xi = 0;\ \tau > 0 \qquad \text{(A6)}$$

In order to solve (A4), we define the functions G and W as

$$G(\omega,\xi,\xi') = \frac{1}{2\sqrt{\pi\omega}}\left[\exp\left\{-\frac{(\xi-\xi')^2}{4\omega}\right\} - \exp\left\{-\frac{(\xi+\xi')^2}{4\omega}\right\}\right] \qquad \text{(A7)}$$

$$W(\tau,\theta,\theta',\varphi,\varphi') = \sum_{l,k} \exp\{-\tau l(l+1)\}\ Y_l^{(k)}(\theta,\varphi)\, Y_l^{(k)}(\theta'\varphi') \qquad \text{(A8)}$$

in which $Y_l^{(k)}$'s are spherical surface harmonics. Function (A7) has the properties

$$G(\omega,0,\xi') = G(\omega,\xi,0) = 0, \quad \frac{\partial G}{\partial \omega} = \frac{\partial^2 G}{\partial \xi^2} = \frac{\partial^2 G}{\partial \xi'^2} \text{ and}$$

$$\lim_{\omega\to 0}\int_0^\infty G(\omega,\xi,\xi')g(\omega,\xi')d\xi' = g(0,\xi) \qquad \text{(A9)}$$

for any bounded continuous function $g(\omega, \xi)$ such as $g(\omega, 0) = 0$. Function (A8) is the fundamental solution of the following differential equation on the unit sphere

$$\frac{\partial H}{\partial \tau} = \Delta H$$

and W has the properties

$$\frac{\partial W}{\partial \tau} = \Delta W = \Delta' W \text{ where } \Delta' W = \frac{1}{\sin\theta'}\frac{\partial}{\partial \theta'}\left(\sin\theta'\frac{\partial W}{\partial \theta'}\right) + \frac{1}{\sin^2\theta'}\frac{\partial^2 W}{\partial \varphi'^2}$$

$$\lim_{\tau\to 0}\iint_S W(\tau,\theta,\theta',\varphi,\varphi')H(\tau,\theta',\varphi')dS' = H(0,\theta,\varphi)$$

for any continuous function $H(\tau,\theta,\varphi)$, and

$$\iint_S W(\tau,\theta,\theta',\varphi,\varphi')dS = \iint_S W(\tau,\theta,\theta',\varphi,\varphi')dS' = 1 \qquad \text{(A10)}$$

where S is the unit sphere, $dS = \sin\theta d\theta d\varphi$, and $dS' = \sin\theta' d\theta' d\varphi'$ which is an area element on the unit sphere.

Now we consider the differential equation

$$\frac{\partial^2 h}{\partial \xi^2} - A\tau\frac{\partial h}{\partial \theta} = 0 \qquad \text{(A11)}$$

The solution of this equation, which satisfies the conditions $h = 1 + \xi$ when $\theta = 0$, and $h = 0$ when $\xi = 0$, $\theta \neq 0$, is given by

$$h = \int_0^\infty G\left(\sqrt{\frac{\theta}{A\tau}},\xi,\xi'\right)(1+\xi')d\xi' = \frac{2}{\sqrt{\pi}}\int_0^{\xi\sqrt{A\tau/\theta}/2}\exp(-\lambda^2)d\lambda + \xi \qquad \text{(A12)}$$

If we put $g = f - h$, we obtain the following equation for g from (A4) and (A11)

$$\frac{\partial g}{\partial \tau} = \frac{\partial^2 g}{\partial \xi^2} + \Delta g - A\tau\frac{\partial g}{\partial \theta} + \Delta h - \frac{\partial h}{\partial \tau} \qquad \text{(A13)}$$

The initial and boundary conditions for this equation are

$$g = 1 \text{ when } \tau = 0 \qquad \text{(A14)}$$

$$g = 0 \text{ when } \xi = 0, \tau \neq 0 \text{ (except where } \theta = 0) \qquad \text{(A15)}$$

Now we consider the function

$$\frac{\partial}{\partial \tau'}\iint_S dS'\int_0^\infty G(\tau-\tau',\xi,\xi')W(\tau-\tau',\theta,\theta',\varphi,\varphi')g(\tau',\xi',\theta',\varphi')d\xi' = \iint_S dS'\int_0^\infty GW\left\{-A\tau'\frac{\partial g}{\partial \theta'} + \Delta' h(\tau',\xi',\varphi') - \frac{\partial h(\tau',\xi',\varphi')}{\partial \tau'}\right\}d\xi'$$

By integrating both sides of the above expression from 0 to τ and using (A14), (A15) and the properties of G and W explained above, we obtain

$$g(\tau,\xi,\theta,\varphi) - \int_0^\infty G d\xi' = \int_0^\tau d\tau\iint_S dS'\int_0^\infty\left(-GWA\tau'\frac{\partial g}{\partial \theta} + GW\Delta' h - GW\frac{\partial h}{\partial \tau'}\right)d\xi' \qquad \text{(A16)}$$

and hence

$$\iint_S \frac{\partial g}{\partial \xi} dS = 4\pi \int_0^\infty \frac{\partial G}{\partial \xi} d\xi' + \iint_S dS \int_0^\tau d\tau \iint_S \int_0^\infty \left(- \frac{\partial G}{\partial \xi} W A\tau' \frac{\partial g}{\partial \theta'} + \frac{\partial G}{\partial \xi} W \Delta' h - \frac{\partial G}{\partial \xi} W \frac{\partial h}{\partial \tau'} \right) d\xi' dS' \quad (A17)$$

From (A10) the second term of the right-hand side of the above equation becomes

$$\int_0^\tau d\tau' \iint_S dS' \int_0^\infty \left(- \frac{\partial G}{\partial \xi} A\tau' \frac{\partial g}{\partial \theta'} + \frac{\partial G}{\partial \xi} \Delta' h - \frac{\partial G}{\partial \xi} \frac{\partial h}{\partial \tau'} \right) d\xi'$$

If we define $h(0, \xi) = 1 + \xi$ in (A12), then h is infinitely differentiable on the surface S. Thus $\iint_S \Delta' h \, dS' = 0$. From (A12) we obtain

$$\frac{\partial h}{\partial \tau'} = \frac{\xi}{2} \sqrt{\frac{A}{\pi \theta' \tau'}} \exp\left(- \frac{A\tau' \xi'}{4\theta'} \right) \quad (A18)$$

Except the region of very small τ', (A18) is small. Because we integrate the concentration gradient with respect to time to obtain the average limiting current expression, the effect of the contribution of (A18) at small values of τ' on the final expression can be neglected. Thus we neglect the third term in the brackets of (A17). It can be seen, furthermore, by applying the successive substitution method to equation (A16) that the first term in the brackets of equation (A17) is also small. Thus (A17) can be simplified as

$$\iint_S \frac{\partial g}{\partial \xi} dS = 4\pi \int_0^\infty \frac{\partial G(\tau, \xi, \xi')}{\partial \xi} d\xi' = 4\pi \left\{ \frac{2}{\sqrt{\pi}} \frac{1}{2\sqrt{\tau}} \exp\left(- \frac{\xi^2}{4\tau} \right) \right\}$$

and therefore

$$\iint_S \left(\frac{\partial g}{\partial \xi} \right)_{\xi = 0} dS = 4 \sqrt{\frac{\pi}{\tau}} \quad (A19)$$

From equation (A12), we obtain

$$\iint_S \left(\frac{\partial h}{\partial \xi} \right)_{\xi = 0} dS = \sqrt{\frac{A\tau}{\pi}} 2\pi \int_0^\pi \frac{\sin \theta}{\sqrt{\theta}} d\theta + 4\pi = 2(1.790)\sqrt{\pi A \tau} + 4\pi \quad (A20)$$

From (A19), (A20) and the relation $f = g + h$ it follows that

$$\iint_S \left(\frac{\partial f}{\partial \xi} \right)_{\xi = 0} dS = \frac{4\pi^{1/2}}{\tau^{1/2}} + 4\pi + 3.580 \, \pi^{1/2} A^{1/2} \tau^{1/2} = \frac{4\pi^{1/2} a}{D^{1/2} t^{1/6}} + 4\pi + \frac{3.580 \pi^{1/2} U_0^{1/2} a^{1/2} t^{1/6}}{3^{1/2} D^{1/2}} \quad (A21)$$

On the other hand, we have

$$\left(\frac{\partial c}{\partial r} \right)_{r = R(t)} = \left(\frac{\partial \xi}{\partial r} \right)_{r = at^{1/2}} \left[\frac{\partial \{ C(1 + \xi)^{-1} f \}}{\partial \xi} \right]_{\xi = 0} = \frac{C}{at^{1/2}} \left(\frac{\partial f}{\partial \xi} \right)_{\xi = 0} \quad (A22)$$

Thus, from (A21) and (A22) we obtain the following expression for the concentration gradient in the radial direction on the surface of the electrode integrated over the total surface area

$$\iint_S \left(\frac{\partial c}{\partial r} \right)_{r = R(t)} \{R(t)\}^2 dS = \frac{C}{at^{1/2}} \iint_S \left(\frac{\partial f}{\partial \xi} \right)_{\xi = 0} (at^{1/2})^2 dS = C \left(\frac{4\pi^{1/2} a^2 t^{1/6}}{3^{1/2} D^{1/2}} + 4\pi a t^{1/2} + \frac{3.580 \pi^{1/2} U_0^{1/2} a^{3/2} t^{1/2}}{D^{1/2}} \right)$$

Therefore the average limiting current is given by

$$i_l = nFCD \frac{1}{t} \int_0^t \left(\frac{4\pi^{1/2} a^2 t^{1/6}}{3^{1/2} D^{1/2}} + 4\pi a t^{1/2} + \frac{(3.580) \pi^{1/2} U_0^{1/2} a^{3/2} t^{1/2}}{D^{1/2}} \right) dt = nFCD^{1/2} \left\{ \frac{(6) 4^{1/2} 3^{1/6} m^{2/3} t^{1/6}}{7\pi^{1/6} d^{2/3}} + \frac{3^{1/2} \pi^{1/2} D^{1/2} (mt)^{1/2}}{4^{1/2} d^{1/2}} + \frac{(3.580) U_0^{1/2} (mt)^{1/2}}{3^{1/2} d^{1/2}} \right\}$$

By putting numerical constants $\pi = 3.1416$, $d = 13.54$ at 25°, we obtain

$$i_l = nFCD^{1/2} \{ 0.238 m^{2/3} t^{1/6} + 2.452 D^{1/2} (mt)^{1/2} + 0.562 U_0^{1/2} (mt)^{1/2} \} \quad (A23)$$

where i_l is expressed in a., C in mole/ml., D in cm.^{2}/sec., m in g./sec., U_0 in cm./sec. and t in sec. Converting the unit of current into μa., and putting $F = 96500$ coulombs, equation 1 is obtained.

Appendix 2 (Case B)

The tangential velocity component in the boundary layer can be written as

$$u = U[2 \{r - R(t)\}/\delta - \{r - R(t)\}^2/\delta^2] \quad (A24)$$

where $\delta = \sqrt{30 \nu R(t) \theta / U}$. The velocity component, v, is given by (A1), and $w = 0$ as in Case A (Appendix 1).

Changing the variables r and t by $\eta = rt^{-1/3}$ and $s = 3t^{1/3}$, equation 4 can be written as

$$\frac{\partial c}{\partial s} = D \left(\frac{\partial^2 c}{\partial \eta^2} + \frac{2}{\eta} \frac{\partial c}{\partial \eta} + \frac{1}{\eta^2} \Delta c \right) - \left(\frac{sv}{3} - \frac{\eta}{s} \right) \frac{\partial c}{\partial \eta} - \frac{su}{3\eta} \frac{\partial c}{\partial \theta} \quad (A25)$$

From (A1), $v \cong 3\eta/s^2$ in the region $r - R(t) << R(t)$ and hence $\eta - a << a$, in which $a = (3m/4\pi d)^{1/3} = R(t)/t^{1/3}$. In addition, $\partial c/\partial t, \partial c/\partial r, \partial^2 c/\partial r^2, \Delta c, \partial c/\partial \theta \cong 0$ outside the range $r - R(t) << R(t)$, and therefore $\partial c/\partial \eta \cong 0$ outside the range $\eta - a << a$. Hence $\left(\frac{sv}{3} - \frac{\eta}{s} \right) \frac{\partial c}{\partial \eta} \cong 0$ in equation (A25). Putting $\eta c(s, \eta, \theta, \varphi) = f(s, \eta, \theta, \varphi)$, equation (A25) becomes

$$\frac{\partial f}{\partial s} = D \left(\frac{\partial^2 f}{\partial \eta^2} + \frac{1}{\eta^2} \Delta f \right) - \frac{su}{3\eta} \frac{\partial f}{\partial \theta}$$

In the vicinity of $r \cong R(t)$, $\eta \cong a$. If we put $\xi = \eta - a$, this equation becomes

$$\frac{\partial f}{\partial s} = D \left(\frac{\partial^2 f}{\partial \xi^2} + \frac{1}{a^2} \Delta f \right) - \frac{su}{3a} \frac{\partial f}{\partial \theta} \quad (A26)$$

By transforming the variables as above, the initial and boundary conditions 15, 16 and 17 can be written as

$$f(0, \xi, \theta, \varphi) = (a + \xi) C \quad (A27)$$

$$f(s, 0, \theta, \varphi) = 0 \text{ when } s > 0 \quad (A28)$$

$$f\{s, \delta(s, \theta), \theta, \varphi\} = \{a + \delta(s, \theta)\} C \quad (A29)$$

where

$$\delta(s, \theta) = \sqrt{90 \nu a \theta / U s}$$

In order to obtain a solution of equation (A26), first we consider the differential equation

$$D \frac{\partial^2 h}{\partial \xi^2} - \frac{su}{3a} \frac{\partial h}{\partial \theta} = 0 \quad (A30)$$

A solution of this equation must satisfy the conditions

$$h(s,0,\theta) = 0 \quad \text{(A31)}$$

$$h\{s,\delta(s,\theta),0\} = \{a + \delta(s,\theta)\}C \quad \text{(A32)}$$

$$\frac{\partial h}{\partial \theta} \cong 0 \text{ except when } \xi << a \quad \text{(A33)}$$

When $\xi << a$, we obtain from (A24)

$$\frac{su}{3a} \cong \frac{s}{3a} U \frac{2U^{1/2}s^{1/2}\xi}{\sqrt{90\nu a\theta}} = \frac{2U^{3/2}s^{1/2}\xi}{\sqrt{810\nu a^3\theta}} = bs^{3/2}\theta^{-1/2}\xi$$

where

$$b = 2U^{1/2}/\sqrt{810\nu a^3} = \text{constant}$$

Therefore, (A30) becomes

$$D\frac{\partial^2 h}{\partial \xi^2} - bs^{1/2}\theta^{-1/2}\xi\frac{\partial h}{\partial \theta} = 0 \quad \text{(A34)}$$

Changing the variables by putting

$$z = (b/D)^{1/3}s^{1/2}\theta^{-1/2}\xi \text{ and } \omega = \theta \quad \text{(A35)}$$

(A34) becomes

$$D^{1/3}b^{2/3}\omega^{-1}\left(\frac{\partial^2 h}{\partial z^2} + \frac{z^2}{2}\frac{\partial h}{\partial z}\right) - b^{2/3}D^{1/3}z\frac{\partial h}{\partial \omega} = 0 \quad \text{(A36)}$$

A particular solution of (A36) can be obtained by substituting h, which satisfies the equation

$$\frac{\partial^2 h}{\partial z^2} + \frac{z^2}{2}\frac{\partial h}{\partial z} = 0$$

by z given by (A35). It is

$$h(s,\xi,\theta) = A\int_0^z \exp\left(-\frac{\zeta^3}{6}\right)d\zeta + B = A_1\gamma(1/3, bs^{3/2}\xi^3/6D\theta^{3/2}) + B \quad \text{(A37)}$$

where A, A_1 and B are constants, and

$$\gamma(X,Z) = \int_0^Z e^{-\zeta}\zeta^{X-1}d\zeta$$

which is an incomplete gamma function. Since (A37) is a particular solution

$$h(s,\xi,\theta) = A_1\gamma(1/3, bs^{3/2}\xi^3/6D\theta^{3/2}) + A_2\xi + B \ (A_2\text{:const.}) \quad \text{(A38)}$$

is also the same. From (A31), (A32), (A33) and (A38), we obtain

$$B = 0$$

and $A_1\gamma(1/3, 30\nu/6D) + A_2\delta(s,\theta) = Ca + C\delta(s,\theta)$. Therefore

$$A_1 = Ca/\gamma(1/3, 30\nu/6D),\ A_2 = C$$

Thus we obtain from (A38)

$$h(s,\xi,\theta) = \frac{Ca\gamma(1/3, bs^{3/2}\xi^3/6D\theta^{3/2})}{\gamma(1/3, 30\nu/6D)} + C\xi \quad \text{(A39)}$$

This is the unique solution of (A30) which satisfies the given conditions.

Next putting $f - h = g$, we can write the following equation from (A26), (A27), (A28) and (A29)

$$\frac{\partial g}{\partial s} = D\left(\frac{\partial^2 g}{\partial \xi^2} + \frac{1}{a^2}\Delta g\right) - \frac{su}{3a}\frac{\partial g}{\partial \theta} + \frac{D}{a^2}\Delta h - \frac{\partial h}{\partial s} \quad \text{(A40)}$$

with the boundary conditions

$$\left.\begin{array}{l} g(0,\xi,\theta,\varphi) = aC,\ (h(0,\xi,\theta) = C\xi \text{ from (A39)}) \\ g(s,0,\theta,\varphi) = 0 \text{ when } s > 0 \\ g\{s,\delta(s,\theta),\theta,\varphi\} = 0 \end{array}\right\} \quad \text{(A41)}$$

In order to solve equation (A40), we define the functions G and W as

$$G(s,\xi,\xi') = \frac{1}{2\sqrt{\pi Ds}}\left[\exp\left\{-\frac{(\xi-\xi')^2}{4Ds}\right\} - \exp\left\{-\frac{(\xi+\xi')^2}{4Ds}\right\}\right] \quad \text{(A42)}$$

$$W(s,\theta,\theta',\varphi,\varphi') = \sum_{l,k}\exp\left\{-\frac{Ds}{a^2}l(l+1)\right\} - Y_l^{(k)}(\theta,\varphi)\,Y_l^{(k)}(\theta',\varphi') \quad \text{(A43)}$$

in which $Y_l^{(k)}$'s are spherical surface harmonics. Functions (A42) and (A43) have the properties similar to (A7) and (A8) in Appendix 1.

With reference to f we can ignore the slight discontinuity at $\xi = \delta(s,\theta)$ when it is integrated to obtain (A44); and h is a smooth function over the whole region. Therefore, from $f - h = g$, g can be regarded as a function which can satisfy (A41). Thus

$$\frac{\partial}{\partial s'}\iint_S dS'\int_0^\infty G(s-s',\xi,\xi')W(s-s',\theta,\theta',\varphi,\varphi')g(s',\xi',\theta',\varphi')d\xi'$$
$$= \iint_S dS'\int_0^\infty GW\left\{-\frac{su(s',\xi',\theta')}{3a}\frac{\partial g}{\partial \theta'} + \frac{D}{a^2}\Delta' h(s',\xi',\theta') - \frac{\partial h(s'\xi',\theta')}{\partial s'}\right\}d\xi'$$

By integrating both sides of the above equation from 0 to s and using (A41) and the characteristic properties of G and W, we obtain

$$\iint_S g(s,\xi,\theta,\varphi)dS = 4\pi C\int_0^\infty G(s,\xi,\xi')a\,d\xi' + \int_0^s ds'\int_0^\infty G(s-s',\xi,\xi')d\xi'\iint_S\left\{-\frac{su}{3a}\frac{\partial g}{\partial \theta'} + \frac{D}{a^2}\Delta' h - \frac{\partial h}{\partial s'}\right\}dS' \quad \text{(A44)}$$

In (A44) the term

$$\iint_S\left(-\frac{su}{3a}\right)\frac{\partial g}{\partial \theta'}dS'$$

is negligibly small compared with the first term of the right-hand side, as can be seen by applying the successive substitution method. From the property of the Laplacian on a sphere it follows that

$$\iint_S \Delta' h\,dS' = 0$$

It can be seen that the value of

$$\int_0^s ds'\int_0^\infty G(s-s',\xi,\xi')d\xi'\iint_S\frac{\partial h}{\partial s'}dS'$$

is also negligible as is clear from the fact that the following expression is evaluated to be very small

$$\frac{\partial h}{\partial s} = \frac{C}{\gamma(1/3, 30\nu/6D)}\left\{\exp\left(-\frac{bs^{3/2}\xi^3}{6D\theta^{3/2}}\right)\right\}\frac{3^{3/2}b^{1/2}\xi}{2^{1/3}D^{1/3}s^{1/2}\theta^{1/2}}$$

Thus, (A44) can be simplified as

$$\iint_S g(s,\xi,\theta,\varphi)\,dS \cong 4\pi C\int_0^\infty G(s,\xi,\xi')a\,d\xi' = \frac{4\pi C}{2\sqrt{\pi Ds}}\int_0^\infty\left[\exp\left\{-\frac{(\xi-\xi')^2}{4Ds}\right\} - \exp\left\{-\frac{(\xi+\xi')^2}{4Ds}\right\}\right]a\,d\xi'$$

It follows from this that

$$\iint_S\frac{\partial g(s,0,\theta,\varphi)}{\partial \xi}dS = \frac{4\pi C}{2\sqrt{\pi D^3 s^3}}\int_0^\infty\left\{\exp\left(-\frac{\xi^2}{4Ds}\right)\right\}\xi a\,d\xi = 4\pi aC/\sqrt{\pi Ds} \quad \text{(A45)}$$

On the other hand, we obtain from (A39)

$$\frac{\partial h(s,0,\theta,\varphi)}{\partial \xi} = \frac{Ca}{\gamma(1/3,\ 30\nu/6D)} \frac{3^{2/3}b^{1/3}s^{1/3}}{2^{1/3}D^{1/3}\theta^{1/3}} + C \quad \text{(A46)}$$

Generally, when Z is very large

$$\gamma(X,Z) \sim \Gamma(X) - Z^{X-1}e^{-Z}\{1 + O(1/Z)\}$$

where $\Gamma(X)$ is a gamma function. In our case, $Z = 30\nu/6D = 5 \times 10^{-2}/10^{-5} > 10^3$. Therefore

$$[\Gamma(1/3) - \gamma(1/3,Z)] \sim e^{-1000}$$

Accordingly we can put $\gamma(1/3,\ 30\nu/6D) = \Gamma(1/3)$. Thus from (A46) we obtain

$$\iint_S \frac{\partial h(s,0,\theta,\varphi)}{\partial \xi} dS = \frac{3^{2/3}b^{1/3}s^{1/3}aC}{2^{1/3}\Gamma(1/3)D^{1/3}} 2\pi \int_0^{\pi} \frac{\sin\theta}{\sqrt{\theta}} d\theta + 4\pi C$$

$$= \frac{2^{2/3}3^{1/3}(1.79)\pi b^{1/3}s^{1/3}Ca}{\Gamma(1/3)D^{1/3}} + 4\pi C \quad \text{(A47)}$$

From $c(t,r,\theta,\varphi) = \eta^{-1}f(s,\xi,\theta,\varphi) = (a + \xi)^{-1}f(s,\xi,\theta,\varphi)$ and $f(s,0,\theta,\varphi) = 0$ we can write the relation

$$\left(\frac{\partial c}{\partial r}\right)_{r=R(t)} = \frac{\partial f(s,0,\theta,\varphi)}{\partial \xi} \frac{1}{a} \left(\frac{\partial \xi}{\partial \eta}\right)_{\eta=a} \left(\frac{\partial \eta}{\partial r}\right)_{r=R(t)} =$$

$$a^{-1}t^{-1/3} \frac{\partial f(s,0,\theta,\varphi)}{\partial \xi} = a^{-1}t^{-1/3} \left\{\frac{\partial g(s,0,\theta,\varphi)}{\partial \xi} + \frac{\partial h(s,0,\theta,\varphi)}{\partial \xi}\right\} \quad \text{(A48)}$$

From (A45), (A47) and (A48) we obtain the following expression for the concentration gradient in the radial direction at the surface of the mercury drop integrated over the total surface area

$$\iint_S \left(\frac{\partial c}{\partial r}\right)_{r=R(t)} \{R(t)\}^2 dS = C\left\{\frac{4^{1/3}3^{1/6}m^{2/3}t^{1/6}}{\pi^{1/6}d^{2/3}D^{1/3}} + \frac{2^{4/3}3^{1/3}\pi^{2/3}(mt)^{1/3}}{d^{1/3}} + \frac{3^{7/6}(1.79)\pi^{1/3}U^{1/3}(mt)^{1/3}}{\Gamma(1/3)\ 30^{1/6}\nu^{1/6}d^{1/3}D^{1/3}}\right\} \quad \text{(A49)}$$

where $\Gamma(1/3)$ is equal to 2.680. Using the same numerical constants as for (A23) we obtain the following equation for the average limiting current expressed in terms of amp.

$$i_1 = \frac{1}{t}\int_0^t \left[nFD \iint_S \left(\frac{\partial c}{\partial r}\right)_{r=R(t)} \{R(t)\}^2 dS\right] dt$$

$$= nFCD^{1/3}\{0.238m^{2/3}t^{1/6} + 2.452D^{1/3}(mt)^{1/3} + 0.438U^{1/3}\nu^{-1/6}D^{1/6}(mt)^{1/3}\}$$

The numerical constant of the third term in the brackets corresponds to a parabolic velocity distribution. Converting the unit of current into μa. we obtain equation 18.

MINNEAPOLIS, MINNESOTA

[CONTRIBUTION FROM THE DEPARTMENT OF CHEMISTRY, NEW YORK STATE COLLEGE OF FORESTRY AT SYRACUSE UNIVERSITY]

Addition of Methyl Radicals to Acetylenic Compounds

BY M. GAZITH AND M. SZWARC

RECEIVED JANUARY 5, 1957

The addition of methyl radicals to several acetylenic compounds was investigated. The activation energies of these addition reactions were found to be higher than those observed in the addition reactions involving the corresponding ethylenic compounds. At the same time it was observed that the entropies of activation are also higher in the additions to the acetylenic compounds. The following pair of compounds were compared: acetylene–ethylene, methylacetylene–propylene, dimethylacetylene–the butenes-2, phenylacetylene–styrene, and diphenylacetylene–the stilbenes. It is suggested that the difference in the reactivity of a C≡C triple bond as compared with a C=C double bond arises from two factors. The π electrons in the shorter C≡C bond interact more strongly and consequently higher activation energy is necessary for the addition process which utilizes one of these electrons. On the other hand, the cylindrical symmetry of the C≡C bond leads to higher entropy of activation than the planar symmetry of the C=C double bond.

During the last few years a considerable amount of work has been carried out in these laboratories on the addition of radicals to aromatic and olefinic compounds.[1-6] The reactions investigated are represented by the general equation

$$R + A \longrightarrow R.A$$

where R denotes a radical, A represents a molecule of an aromatic or an olefinic compound, and R.A represents the primary addition product which, of course, is also a radical. Most of these investigations dealt with the addition of methyl radicals, and the relative rate constants of such additions, denoted as methyl affinities, were measured by the ratios k_2/k_1, where the subscripts refer to the two reactions[7]

$$CH_3 + \text{solvent} \longrightarrow CH_4 + \text{solvent radical} \quad (1)$$

$$CH_3 + A \longrightarrow A.CH_3 \quad (2)$$

The investigation reported in the present communication deals with the addition of methyl radicals to acetylenic compounds. The main purpose of this study was to find how the reactivity of a C≡C triple bond differs from that of a C=C double bond, and to interpret this difference in terms of electronic structures of the respective compounds.

Experimental

The following acetylenic compounds were investigated: acetylene, methylacetylene, dimethylacetylene, phenylacetylene, diphenylacetylene, and dimethyl ester of acetylene dicarboxylic acid. Acetylene was purchased from Matheson Co. and was 99.5% pure. The gas was deaerated and then distilled from trap to trap, the middle portion being collected. In some experiments the gas used was twice distilled. This additional purification did not affect the results indicating that our rate constants for acetylene are genuine.

High purity grade methylacetylene and dimethylacetylene were obtained from Farchan Research Laboratories. These compounds were used without further purification. Phenylacetylene and diphenylacetylene were prepared and purified by Dr. Bader from Aldrich Chemicals.[8] Finally, the dimethyl ester of acetylene dicarboxylic acid was prepared in our laboratories from the respective dicarboxylic acid. The ester was purified by fractionation *in vacuo*.

(1) M. Levy and M. Szwarc, THIS JOURNAL, 77, 1949 (1955).
(2) M. Szwarc, *J. Polymer Sci.*, 16, 89 (1955).
(3) A. Rembaum and M. Szwarc, THIS JOURNAL, 77, 4468 (1955).
(4) F. Leavitt, M. Levy, M. Szwarc and V. Stannett, *ibid.*, 77, 5493 (1955).
(5) R. P. Buckley and M. Szwarc, *ibid.*, 78, 5696 (1956).
(6) J. Smid and M. Szwarc, *ibid.*, 78, 3322 (1956).
(7) The same solvent was used in each series of investigated compounds A's. Hence, k_1 remains constant throughout the series.

(8) We take this opportunity to thank Dr. Bader for his assistance.